Upper Ocean Thermal Structure and the Western North Pacific Category-5 Typhoons Part II: Dependence on Translation Speed

I-I Lin, Iam-Fei Pun, and Chun-Chieh Wu

Dept. of Atmospheric Sciences, National Taiwan University, Taipei, Taiwan

Revised and Submitted to the Monthly Weather Review

December 8, 2008

Corresponding author address: Dr. I-I Lin, Dept. of Atmospheric Sciences, National Taiwan University, No. 1, Sec. 4, Roosevelt Rd., Taipei 106, Taiwan; e-mail: iilin@as.ntu.edu.tw

Abstract

Using new *in situ* ocean subsurface observations from the Argo floats, best track typhoon data from the U.S. Joint Typhoon Warning Center, an ocean mixed layer model and other supporting data sets, this work systematically explore the inter-relationships between translation speed, ocean's subsurface condition (characterized by the depth of the 26° C isotherm (D26) and upper ocean heat content (UOHC)), cyclone's self-induced ocean cooling negative feedback, and air-sea enthalpy fluxes for the intensification of the western North Pacific category-5 typhoons.

Based on 10 years' analysis, it is found that for intensification to category-5, in addition to the warm sea surface temperature generally around 29° C, the required subsurface D26 and UOHC depend greatly on cyclone's translation speed. It is observed that even over relatively shallow subsurface warm layer of D26~ 60-70 m and UOHC ~ 65-70 kj cm^{-2}, it is still possible to have sufficient enthalpy flux to intensify to category-5, provided that the storm can be fast-moving (typically U_h ~ 7-8 m s^{-1}). On the contrary, a much deeper subsurface layer is needed for slow-moving typhoons. For example at U_h ~ 2-3 m s^{-1}, D26 and UOCH are typically ~ 115-140 m and ~ 115-125 kj cm^{-2}, respectively.

A new concept named as the 'affordable minimum translation speed, U_{h_min}' is proposed. This is the minimum required speed a storm needs to travel for its intensification to category-5, given the observed D26 and UOHC. Using more than 3,000 Argo *in situ* profiles, series of mixed layer numerical experiments are conducted to quantify the relationship between D26, UOHC and U_{h_min}. Clear negative linear relationships with correlation coefficients R= -0.87 (-0.71) are obtained as $U_{h\_min} = -0.065 \times D26 + 11.1$, and $U_{h\_min} = -0.05 \times UOHC + 9.4$, respectively. These relationships can thus be used as a guide to predict the minimum speed a storm has to travel at for intensification to category 5, given the observed D26 and UOHC.

1. Introduction

a. Motivation

Category-5[1] tropical cyclones are the most intense and damaging cyclones on earth. Why these storms can reach such extraordinary intensity has been an intriguing and challenging research topic because intensification is a complex process involving multiple interactions among the cyclone, ocean, and atmosphere (Gray 1977; Merrill 1988; Emanuel 1995; 1997; 1999; 2005; Shay et al. 2000; Frank and Ritchie 2001; Emanuel et al. 2004; Lin et al. 2005; 2008a;b; Tremberth 2005; Montgomery et al. 2006; Houze et al. 2007; Vimont and Kossin 2007; Black et al. 2007; Vecchi and Soden 2007; Wu et al. 2007; Mainelli et al. 2008). To reach such high intensity, multiple conditions from both atmosphere (e.g., vertical wind shear and high level outflow; Frank and Ritchie 2001; Wang and Wu 2003; Emanuel et al. 2004) and ocean all have to be favourable. Also, since ocean is the energy source for intensification, it is a necessary condition (Emanuel 1995; 1997; 1999; Shay et al. 2000; Emanuel et al. 2004; Lin et al. 2005; 2008a;b; Tremberth 2005; Black et al. 2007). Thus, even if all other conditions are favourable, without satisfying the ocean condition it is not possible for the intensification to take place.

When considering the ocean condition, both sea surface temperature (SST) and the subsurface thermal structure are important because cyclones interact not only with the ocean surface, but with the entire upper ocean column (typically from surface down to 100-200m) (Perlroth 1967; Leipper and Volgenau 1972; Gray 1979; Holliday and Thompson 1979; Shay et al. 2000; Cione and Uhlhorn 2003; Goni and Trinanes 2003; Lin et al. 2005; 2008a;b; Pun et al. 2007; Wu et al. 2007). However, the lack of subsurface observations has long been a major hindrance to understand the role ocean's subsurface thermal structure play in the intensification of category-5 cyclones.

In recent years, due to the advancement in ocean *in situ* observations (e.g., the deployment of Argo floats, Gould et al. 2004; Roemmich et al. 2004), the situation has improved and new observations are

[1] Saffir-Simpson Tropical Cyclone Scale based on the 1-minute (10-minute) maximum sustained winds: Category-1: 34-43 (30-37) ms^{-1}, Category-2: 44-50 (38-43) ms^{-1}, Category-3: 51-59 (44-51) ms^{-1}, Category-4: 59-71 (52-61) ms^{-1}, and Category-5: > 71 (> 61) ms^{-1}.

now available for research (Johnson et al. 2006; Lyman et al. 2006; Trenberth 2006; Willis et al. 2007). Therefore in Part I (Lin et al. 2008a) of this work, these new subsurface observations are used to explore issues related to ocean features, while in this work (Part II) the focus is on exploring issues related to cyclone's translation speed. As in Part I, western North Pacific typhoons are studied because this area is where most category-5 cyclones occur on earth.

b. Issues on the translation speed

In extant literatures, it is generally known that if a cyclone is to reach high intensity such as category 5, in addition to warm SST, a sufficiently thick layer of warm water below the surface is also required as a necessary pre-condition (Leipper and Volgenau 1972; Gray 1979; Holliday and Thompson 1979; Emanuel 1999; Shay et al. 2000; Cione and Uhlhorn 2003; Emanuel et al. 2004; Lin et al. 2005; 2008a). This is required because it will ensure the negative feedback from cyclone's self-induced SST cooling to be restrained during the intensification. Otherwise, the self-induced cooling would be too strong for continual intensification to category 5 since self-induced cooling reduces the available air-sea flux supply for intensification (Price 1981; Gallacher et al. 1989; Emanuel 1999; Cione and Uhlhorn 2003; Emanuel et al. 2004; Lin et al. 2005; 2008a;b; Wu et al. 2007). As reported in Gallacher et al. 1989; Emanuel (1999) and Emanuel et al. (2004), a mere 2.5° C cooling in the inner-core is already sufficient to shut-down the entire energy production of a storm. An interesting question one may ask is how thick the subsurface warm layer is to be considered as thick enough? In other words, what is the needed range for the subsurface parameters, such as the depth of the 26°C isotherm (i.e., D26, often used to characterize the subsurface warm layer thickness) or the upper ocean heat content (UOHC or Q_H, i.e., the integrated heat content excess per unit area relative to the 26°C isotherm, integrated from D26 to the surface)[2]

[2] $Q_H = c_p \rho \sum_{i=1}^{n} \Delta T(x, y, z_i, t) \Delta Z$ where c_p is the capacity heat of the seawater at constant pressure taken as 4178 J kg^{-1}°C^{-1}, ρ is the average seawater density of the upper ocean taken as 1026 kg m^{-3}, $\Delta T(x, y, z_i, t)$ is the temperature

(Leipper and Volgenau 1972; Shay et al. 2000; Goni and Trinanes 2003; Pun et al. 2007; Lin et al. 2008a;b; Mainelli et al. 2008)? Meanwhile, since ocean's negative feedback is weaker when a storm is fast-moving, will the requirements for fast or slow-moving storms be different? It has been hinted in Part I (Lin et al. 2008a) that some faster-moving storms were observed to intensify to category 5 over relatively shallow layer of warm water. As such, this study aims to systematically investigate and quantify the relationship between translation speed and the required subsurface parameters.

In Section 2, we first examine the relationship between the observed translation speed and upper ocean thermal structure (UOTS) in the intensification locations of category-5 typhoons. Data from the recent 10 years (1997-2006) are studied because prior to 1997, very limited *in situ* UOTS data are available. Typhoon's translation speed, track, and intensity data are taken from the best track data of the Joint Typhoon Warning Center (JTWC). The *in situ* UOTS data are obtained from the NOAA GTSPP (Global Temperature and Salinity Profile Program) (Keeley et al. 2003) and the Argo[3] float data bases (Gould et al. 2004; Roemmich et al. 2004; Lyman et al. 2006; Willis et al. 2007). Next, the during-storm self-induced cooling negative feedback is estimated under various translation speeds and subsurface conditions using the Price-Weller-Pinkel (PWP) ocean mixed layer model (Price et al. 1986). Air-sea enthalpy fluxes are also estimated accordingly (Powell et al. 2003; Black et al. 2007; Lin et al. 2008a;b).

In section 3, a new concept called the 'affordable minimum translation speed (U_{h_min})' is proposed. This is the minimum speed a storm has to travel to confine the self-induced cooling within a certain threshold during the intensification process to category 5, given the observed subsurface D26. Using more than 3,000 Argo profiles (Gould et al. 2004; Roemmich et al. 2004; Lyman et al. 2006; Willis et al. 2007) to conduct a series of mixed layer model experiments, relationship between D26 and U_{h_min} is

---

difference between $T(z_i)$ and 26℃ at depth z_i, and ΔZ is the depth increment taken as 5m. n is the total layers from surface to the depth of 26℃ (D26). The total UOHC is the sum of UOHC at each depth increment (ΔZ) through the surface to the D26.

[3] In this work, all Argo profiles are pre-screened to ensure data quality. As reported by Willis et al. (2007), a small subset of floats fabricated at the Woods Hole Oceanographic Institution was detected to have cold-bias. Thus, data from this batch of floats is screened out and not used in this study.

established. In Section 4, similar relationships are established for UOHC and U_{h_min}. In Section 5, issues related to future forecasts and ocean features (i.e., consolidating results with Part I, Lin et al. 2008a), and concerns of other factors (e.g., stratification) in future research are discussed. Conclusions are given in Section 6.

2. UOTS – *Uh* relationship observed during 1997-2006 together with the associated self-induced cooling and enthalpy flux

a. The observed UOTS-Uh relationship

Fig. 1a depicts the *in situ* upper ocean thermal structure profiles found in the intensification locations (from category 1 to the peak in category 5) of category-5 typhoons during the May-October typhoon season in the recent 10 years. Profiles are searched within 8 days prior to the passage of each storm and within 2 degree radius from the best-track. 17 Profiles from 13[4] out of the 25 category-5 typhoons are found.

As in Fig. 1a, SST values are confined within a narrow range between 28 and 30° C while large variability is found in the subsurface. Namely, the depth of the 26° C isotherm ranges from as shallow as 58m to as deep as 150m (i.e.~ 200% difference). Based on the differences in D26, the *in situ* profiles can be categorized into 5 groups, from the shallowest G1 (D26= 45-65m) to the deepest G5 (D26= 125-150m) (Fig. 1a). As summarized in Table 1, the average SST is similar among the 5 groups with values all near 29° C. In contrast, distinct differentiation can be seen in the 2 subsurface parameters that the average D26 increases from 61 in G1 to 138m in G5 while UOHC from 64 to 122 kj/cm^2.

Examining the observed translation speed[5] for the 5 groups (Fig. 1b), one finds that shallower layers

[4] These 13 category-5 typhoons are: Saomai (2006), Yagi (2006), Nabi (2005), Dianmu (2004), Chaba (2004), Maon (2004), Maemi (2003), Hagibis (2002), Fengshen (2002), Bilis (2000), Saomai (2000), Nestor (1997), and Joan (1997). For the case of Saomai (2006), Yagi (2006), Maemi (2003), and Fengshen (2002), two profiles are found while one profile is found for the other storms. Thus, there are altogether 17 profiles.

[5] For each profile, the corresponding translation speed is calculated from the nearest point in the track.

(G1 and G2) are associated with faster translation speed (~ 7.3-8.5m s^{-1}) while over deeper waters (e.g., G4 and G5), wider range of translation speed is found, i.e., from the slowest 2.6 m s^{-1} to 6.4 m s^{-1}. Also in Table 1 and Fig. 1b, one observes that with increase in D26 and UOHC from G1 to G5, the observed minimum *Uh* of each group decreases. These suggest that deeper warm layers (e.g., G4 and G5) allows a storm to intensify to cateogory5 under both slow (e.g., ~ 2.6 m s^{-1}) and fast (e.g., ~ 6.4 m s^{-1}) translation speeds, i.e., allowing a wider range of *Uh* for a storm to travel. However, over shallower warm layer (e.g., G1 and G2), a storm is only allowed to travel fast (i.e., 7.3-8.5 m s^{-1}) and the range of *Uh* a storm is allowed to travel is also smaller (Fig. 1b).

b. Estimation of self-induced SST cooling

To further confirm the observed *Uh* and UOTS relationship, a mixed layer model is run for each of the 5 groups. As in Part I, the PWP ocean mixed layer model (Price et al. 1986) is used. The corresponding *in situ* profiles for each group (Fig. 1a) are used as initial profiles (Fig. 1a). For each profile, the storm-induced cooling at the inner core is estimated progressively with increase in wind forcing from category-1 to 5. Thus for each profile, the 10-minute average maximum sustained wind, ranging from 30-65 m s^{-1}, at every 5 m s^{-1} interval, is used to drive the model. The drag coefficient used is the cyclone-wind drag coefficient (*Cd*) from Powell et al. (2003). Also, according to *Uh*, a model parameter called $TC_{transit-time}$ is calculated and the model is run according to the $TC_{transit-time}$ where $TC_{transit-time}$ = D/*Uh* (D : inner core diameter of the storm). More details of the model set up can be found in Part I (Lin et al. 2008a). Fig. 2 depicts the numerical results of the group-averaged during-storm inner-core SST due to the self-induced cooling for each of the 5 groups according to the observed translation speeds (Fig. 1b).

One can see that for all 5 groups the self-induced cooling is similar and well-restrained during the intensification period. Even at category-4 and 5, the during-storm SST is still around 27-28° C, corresponding to only around 1-2° C reduction from the pre-storm SST of around 29° C (Figs. 2, 3, and

Table 2). It can be questioned why over shallow layers (i.e. G1 and G2) the self-induced cooling can be restrained and similar to the values as those cases passing over the deeper layers (i.e., G4 and G5)?

From Fig. 4 one can see that this is due to the differences in translation speed. In Figs. 4a and b, it can be found that though over shallow layers, the corresponding translation speeds are fast (i.e., 7.9-8.5 m s^{-1} for G1 and 7.3-8.2 m s^{-1} for G2, see Fig. 1b). As a result, the self-induced cooling (i.e. shaded regions in Figs. 4a and b) is comparable to the cooling over deeper layers (i.e., shaded regions in Figs. 4d and e) under slow or moderate *Uh* (i.e., 2.6-6.4 for G4 and 2.9-4.8 for G5, Fig. 1b). These illustrate the compensation effect of the translation speed that even if a storm passes over shallow warm layer, it can still be compensated by its fast translation speed to limit the self-induced cooling during the intensification process.

c. Enthalpy flux estimation

In order to evaluate the difference in the available air-sea enthalpy (latent + sensible heat) flux due to difference in the translation speed during the intensification process, for each group the inner-core sensible (Q_S) and latent heat fluxes (Q_L) are calculated using the bulk aerodynamic formulae (Jacob et al. 2000; Cione and Uhlhorn 2003; Powell et al. 2003; Black et al. 2007) as follows:

$$Q_S = C_H W (T_s - T_a) \rho_a C_{pa}, \qquad (1)$$

$$Q_L = C_E W (q_s - q_a) \rho_a L_{va}, \qquad (2)$$

where C_H and C_E are the sensible and latent heat exchange coefficients; W is the wind speed; T_s and T_a are SST and near surface air temperature; q_s and q_a are surface and air specific humidity; ρ_a, C_{pa}, and L_{va} are air density, heat capacity of the air, and latent heat of vaporization. In this work, the exchange coefficients are from Black et al. (2007). Corresponding to the self-induced cooling (Fig. 4), fluxes are estimated progressively at every 5 m s^{-1} interval wind speed from category-1 to 5, so as to cover the complete range of intensification. The near surface atmospheric temperature and humidity data is from the 1.125° resolution data (ERA 40) of the ECMWF (European Center for Medium Range

Weather Forecast). Thus for each typhoon case in the group, the corresponding ERA 40 data is used. Also the corresponding SST data for each typhoon case in the group is from the output of the mixed layer model (Section 2b) so that the self-induced cooling effect during the intensification process can be incorporated. As in Fig. 4, the during-storm available enthalpy fluxes for each group under various translation speeds (i.e., Uh=1, 2, 3……10 m s^{-1}) are estimated.

Fig. 5 depicts the averaged available enthalpy flux at inner core for each group. It can be seen that the flux condition is consistent with the self-induced cooling results that even over shallow waters like G1 and G2, there can still be sufficient flux available during intensification, as long as the translation speed is fast enough. One can see that with the observed Uh of about 7.9-8.5 m s^{-1} for G1 (shaded region in Fig. 5a) and Uh of 7.3-8.2 m s^{-1} for G2 (shaded region in Fig. 5b), the available flux is comparable to the available flux over deeper waters under moderate or slow speed (e.g. shaded regions in Figs. 5d and 5e where Uh = 2.6-6.4 m s^{-1} for 5d and Uh = 2.9-4.8 m s^{-1} for 5e). Typically at category 1 and 2, enthalpy flux is around 500-700 W m^{-2}, at category 3, ~ 800-900 W m^{-2} and at category 4 and 5, around 1,000-1,500 W m^{-2}. It can also be seen in Figs. 5a and b that if passing shallow warm layer at moderate or slow speed (e.g., Uh = 1-4 m s^{-1}), it is not possible to intensify to category 5 because the available enthalpy flux is around zero before reaching category 5.

3. Concept of the affordable minimum translation speed (U_{h_min}) and the minimum D26 ($D26_{\_min}$)

From above, one sees that a shallow warm layer allows a storm to intensify to category 5 only under fast translation speed. Over deeper warm layer, a storm is allowed to travel much slower and can intensify to category-5 under both fast and slow translation speeds. As such, it will be useful to identify a critical minimum translation speed for each specific warm layer. Thus in this work, a new concept, 'affordable minimum translation speed, U_{h_min}', is proposed. This is the critical minimum speed a storm has to travel during its intensification process to category 5, so that the self-induced SST cooling negative feedback can be restrained within a chosen threshold, given an upper ocean thermal profile. As in Fig. 4 and Table 2, 2.2°C is the maximum self-induced cooling found during the intensification process among

all the category-5 typhoons over the past 10 years, thus threshold of 2.2°C is used..

This concept can be explained using examples in Fig. 6. Given 2 profiles of similar SST values (both ~ 29.7°C) but of different warm layer thickness, one over shallow D26 of 67m (Profile 1) and the other over deep D26 of 134m (Profile 2), the self-induced cooling results are very different (Fig. 6b for Profile 1 and Fig. 6c for Profile 2). As in Fig. 6b, over the shallow warm layer, a storm has to travel at a speed 8 m s^{-1} to prevent the self-induced SST cooling from falling below the threshold (i.e., to be confined within the light grey-shaded region). However, if over the deep warm layer, a storm can afford to travel more slowly, as at a speed 4 m s^{-1}, to keep the self-induced cooling restrained (i.e., within the light grey-shaded region in Fig. 6c). Therefore for Profile 1, U_{h_min} is 8 m s^{-1} while for Profile 2, U_{h_min} is reduced to 4 m s^{-1}.

Applying this concept and run mixed layer model (Price et al. 1986) to profiles in Fig. 1a under various U_h (i.e., 1, 2, …. 10 m s^{-1}), respective U_{h_min} for each profile is identified. As depicted in Fig. 7a, clear negative dependence between D26 and U_{h_min} is found, with correlation coefficient R of -0.86. To further confirm this relationship, the 17 profiles in Fig. 1a are too few in number and more profiles are needed. Therefore, we search from the Argo data base (Gould et al. 2004; Roemmich et al. 2004) all available *in situ* profiles found in the region between 120-170°E and 10-26°N (boxed region in Fig. 8a) because this is the observed intensification domain for category-5 typhoons, as identified in Part I (Lin et al. 2008a). As Argo floats became available in 2000 (Gould et al. 2004), all typhoon season (May-October) profiles from 2000 to 2006 are searched. Also from Fig. la and Table l, 28°C is the minimum observed value for SST in the intensification locations of category-5 typhoons, profiles of 28°C are used. In total, 3326 profiles are identified, as depicted in Fig. 8b (grey profiles). It can be seen in Fig. 8a that though these profiles may not be the ones found directly along the track of historical category-5 typhoons (i.e., the profiles in Fig. 1a), they are still the valid 'candidate' profiles for possible intensification to category-5 because they are from the same intensification region during the typhoon season. It can be observed in Fig. 8b that the depth-temperature distribution of these profiles is similar

and consistent to the ones found along the track.

Running the mixed layer model to these > 3000 profiles, U_{h_min} for each profile is identified. As depicted in Fig. 7b, similar negative dependence between D26 and U_{h_min} is found, with correlation coefficient R of -0.87. Applying the least square fit over these 3326 D26-U_{h_min} pairs, a first-order relationship between D26 and U_{h_min} is obtained as:

$$U_{h\_min} = -0.065 \times D26 + 11.1 \quad (3)$$

This provides a simple way to quantify the minimum translation speed required during intensification to category-5, given D26. In addition, since Fig. 7b depicts a linear dependence, it can also be used to estimate the required minimum D26 (i.e., $D26_{\_min}$), if given U_h (Fig. 7c), as:

$$D26_{\_min} = -11.7 \times U_h + 155 \quad (4)$$

From above, it can be seen that how thick the subsurface warm layer required for intensification to category-5 is a sensitive function to translation speed and the requirements between fast and slow-moving storms are different.

Testing the validity of the relationships in eqns. (3) and (4) using the actual 10 years' observations in Section 2a, one can see that this new concept is supported by the observations. As in Table 1, the averaged observed D26 for Group 1-5 are 61m, 73m, 93m, 116m, and 138m, respectively. Using eqn. 3, one can calculate the corresponding U_{h_min} = 2 m s^{-1}, 3.5 m s^{-1}, 5m s^{-1}, 6.3m s^{-1}, and 7 m s^{-1}. Therefore, one can see that if a storm is to intensify to category-5 over the shallowest G1 waters, it needs to transverse at a speed 7 m s^{-1}. Examining the observed U_h range for G1, one sees that it fell between 7.9-8.5 m s^{-1} (Table 1 and Fig. 1b), i.e., in good agreement with the estimated U_{h_min} of 7 m s^{-1}. Checking the other 4 groups, similar agreements are also found. For example over the G5 waters, the observed range of U_h is 2.9-4.8 m and the U_{h_min} = 2 m s^{-1} (Table 1 and Fig. 1b).

Next, eqn. (4) is tested. As in Table 1, the observed averaged U_h for G1 to G5 are 8.2 m s^{-1}, 7.8 m s^{-1}, 5.6 m s^{-1}, 4.5m s^{-1}, and 4.1 m s^{-1}. Using eqn. (4), the corresponding $D26_{\_min}$ is estimated to be 59m, 64m, 89m, 102m, and 107m, respectively. Examining the observed averaged D26, indeed they satisfy

this required minimum and the corresponding observed averaged D26 are 61m, 73m, 93m, 116m, and 138m, i.e., $D26_{\_min}$. Therefore, eqns. (3) and (4) can be used to quantify the minimum subsurface requirements for intensification to category-5. If given the observed translation speed, one can estimate the required minimum D26 using eqn. (4). Reversely, if given the observed D26, eqn. (3) can be used to estimate the required minimum *Uh*.

4. Affordable minimum translation speed and the minimum upper ocean heat content

Besides from D26, another subsurface parameter of interest is the upper ocean heat content (Leipper and Volgenau 1972; Shay et al. 2000; Goni and Trinanes 2003; Pun et al. 2007; Lin et al. 2008a;b). Using the more than 3000 *in situ* Argo profiles in Fig. 8b, UOHC is calculated. First, UOHC is compared with D26. As shown in Fig. 9a, UOHC is highly correlated with D26, with R=0.86. Examining the UOHC for each profile with the corresponding U_{h_min}, similar dependence (R= -0.71) is found as D26 and U_{h_min}. Therefore similar to results presented in Section 3, simple linear relationships (Figs. 9b and 9c) are obtained as:

$$U_{h\_min} = -0.05 \times UOHC + 9.4 \qquad (5)$$

$$UOHC_{\_min} = -10.1 \times U_h + 142 \qquad (6)$$

Also, it should be clarified that the 'lower UOHC' stated above is referred to the situation of shallow subsurface warm layer and not referred to as a SST reduction situation. Since UOHC is integrated from surface (SST) down to D26, therefore besides from shallow subsurface warm layer, low SST also can cause low UOHC. However, from Figs. 1a, 8b and Table 1, the pre-storms SSTs in this work are all $\geqq$ 28°C, i.e., warm SST is a pre-requisite (based on 10 years' *in situ* observations in Section 2) to be considered before meeting the subsurface condition (i.e., D26 and UOHC). As such, the referred 'lower UOHC' in the context of this study is related to as shallow subsurface warm layer, not as reduction in SST.

5. Discussions

a. Suggestion for future forecast reference

In recent years, there is an increasing demand to incorporate the subsurface information like D26 and UOHC as one of the forecast indicators (Shay et al. 2000; Goni and Trinanes 2003; Lin et al. 2005; 2008a;b; Pun et al. 2007). From the results of this work, one can see that since the subsurface requirements for fast and slow-moving storms are different, it will be more accurate to consider the subsurface parameters with respect to the translation speed. For example, convenient look up tables (LUTs) can be generated from Figs. 7c and 9c so that given a storm's observed or predicted *Uh*, the required minimum D26 and UOHC can be used to test whether the actual subsurface warm layer is thick enough to satisfy the minimum requirement. As in Tables 3 and 4, given U_h = 1-3, 4-6, and 7-9 ms^{-1}, the corresponding average $D26_{\_min}$ ($UOHC_{\_min}$) is about 124-144m (116-122 kj cm^{-2}), 76-107m (75-104 kj cm^{-2}), and 56-68m (56-66 kj cm^{-2}), respectively. Also in Tables 3 and 4, standard deviations are given, so as to provide reference to account for the spreading observed in Figs. 7c and 9c.

b. Inter-relationship with ocean features

In Part I (Lin et al. 2008a), the role ocean features (i.e., the positive or negative sea surface height anomaly (SSHA) features detected from satellite altimetry) play in the intensification of category-5 typhoons is discussed. Consolidating the results found in this work and Part I, the inter-relationship between translation speed, feature encountering, and subsurface warm layer in category-5 typhoon's intensification is discussed as follows. Basically it is a matter of meeting the minimum subsurface requirement established in this work and 3 factors are involved, i.e., translation speed, the background climatological UOTS, and the actual *in-situ* UOTS modulated by the presence of the ocean features[6]. If

[6] As explained in Part I, features detected from satellite altimetry represents the deviation of the current *in situ* UOTS from the background climatological UOTS. Therefore there can be 3 possible scenarios: a. + SSHA feature scenario (i.e., deepening of the subsurface warm layer from the climatological background), b. no feature scenario (i.e., no deepening and shoaling, the actual subsurface warm layer is similar to the background), and c. – SSHA feature scenario (i.e., shoaling of the

the observed translation speed is given, the background climatological warm layer is too shallow to meet the minimum requirement, then encountering the positive SSHA feature is needed so that the warm layer can be deepened from the background to meet the minimum.

Using the U_{h_min} concept in this work, Fig. 10 can be used as a reference in guiding the interpretation of feature encountering. Fig. 10 depicts U_{h_min} (annotated in stars) for various background D26 (based on eqn. 3). If the actual $U_h < U_{h\_min}$ (i.e., fall within the range between 0- U_{h_min}, in blue) then encountering the positive SSHA feature is necessary because the storm is not travelling fast enough. On the other hand, if the actual $U_h \geqq U_{h\_min}$ (in green), then encountering of the positive SSHA feature is not necessary. Also from Fig. 10, the applicable range for the 3 sub-regions (i.e., SEZ, Kuroshio, and gyre central) in the North western Pacific identified in Part I are depicted. It can be clearly seen that the shallower the background (e.g., the SEZ), the larger the corresponding U_{h_min}, the more encountering of the positive SSHA feature (i.e. over wider range of U_h) is needed, and vice versa.

c. Issue on changing the threshold

In this study, because 2.2°C is the maximum self-induced cooling found during the intensification to category-5 in the past 10 years (Table 2), it is used as the threshold value to obtain the minimum translation speed (Sections 3 and 4). If one replaces the threshold using the mean self-induced cooling value of around 1.6°C (i.e., last column in Table 2) instead of 2.2°C and re-do the mixed layer experiments, then the new D26-*Uh* pairs and the regression relationship would be for obtaining the mean translation speed (U_{h_mean}) instead of the minimum. In other words, given D26 or UOHC, U_{h_min} is the minimum speed a storm has to travel to keep the self-induced cooling below the maximum cooling of 2.2°C while U_{h_mean} would be the mean speed a storm travels to keep the cooling at the mean value of around 1.6°C. As can be seen in Fig. 11, the new regression relationship is given as:

$$U_{h\_mean} = -0.06xD26 + 12.1 \quad (7)$$

---

subsurface warm layer from the background climatology).

By comparing the new regression relationship (black-solid curve in Fig. 11a, i.e., eqn. (7)) with the relationship for the U_{h_min} (brown-solid curve in Fig. 11a or black curve in Fig. 7b, i.e., (3)), one can see that given the same D26, $U_{h\_mean} > U_{h\_min.}$. By overlaying the actual observed D26 and *Uh* pairs for the category-5 typhoons in the past 10 years (i.e., from Section 2a), one can see that this mean relationship well matches the actual observations and the regression relationship derived from the actual D26-*Uh* pairs (i.e., the black-dash regression line in Fig. 11a, $U_{h\_obs} = -0.055 \times D26_{\_obs} + 11.3$, eqn. (8)) is almost identical to eqn. (7). Similarly as in Fig. 11b, if given U_h, the corresponding $D26_{\_mean} > D26_{\_min.}$

d. Issues on other factors

Though in this work the focus is on the role of the translation speed, it does not imply that other factors are not important, for example, issues related to typhoon size, ocean's horizontal advection, upwelling, and stratification are also important factors to join in the consideration in the future. For example when considering the thermocline stability below the ocean mixed layer, the Brunt-Vaisala frequency (N^2), can be calculated from the Argo profiles. With this extra information, one can further sub-divide the $D26_{\_min} - Uh$ pairs (i.e., Fig. 7c) into 2 groups, one under the small-regular N^2 condition (here $\leqq 4 \times 10^{-4} S^{-2}$ is used as the criterion, Fig. 12a) while the other under the large N^2 condition (Fig. 12b). Thus, the regression relationships can be obtained separately for these 2 sub-groups. As can be seen in Fig. 12b, under the large N^2 (i.e., more stratified) condition, it does not need as deep the subsurface warm layer to intensify to category-5, e.g., if given $U_h = 5$ ms^{-1}, the corresponding $D26_{\_min}$ is ~ 82m under the large N^2 condition (Fig. 12b) and ~ 99m under the small-regular N^2 condition. This is reasonable since large N^2 is unfavourable for mixing, thus inhibits the self-induced cooling negative feedback. As such, if the N^2 is large, the subsurface warm layer required for intensification to category-5 is not as deep as compared to the small-regular N^2 condition.

Finally, it should also be reminded that ocean's condition (including SST and subsurface) is a necessary but not a sufficient condition in intensification and the focus of this work is to explore the

borderline of ocean's subsurface necessary condition with respect to the translation speed for category-5 typhoons. Certainly it is not possible to reach category 5 without meeting all other favourable atmospheric and storm structure conditions (e.g., Merril 1988; Frank and Ritchie 2001; Wang and Wu 2003; Emanuel et al. 2004; Montgomery et al. 2006; Houze et al. 2007; Mainelli et al. 2008).

6. Conclusion

Category-5 cyclones are the most intense cyclones on earth. For long it is known that in addition to warm SST, a sufficiently thick layer of subsurface warm water is also required as a necessary pre-condition for reaching such high intensity (e.g., Leipper and Volgenau 1972; Gray 1979). However, due to the lack of *in situ* observations it has been difficult to quantify how thick the subsurface warm layer is considered as thick enough. With the advancement in *in situ* ocean observations like the deployment of Argo floats (Roemmich *et al.* 2004; Trenberth 2006), it is now possible to take a fresh look at the situation using new observations. Based on 10 years' data, it is found that SST is typically around 29°C. However, the subsurface condition depends strongly on cyclone's translation speed.

It is observed that faster-moving typhoons of $U_h \sim$ 7-8 ms^{-1} can afford to intensify to category-5 over shallow subsurface warm layer characterized by D26 ~ 60-70m and UOHC ~ 65-70kj cm^{-2} while slow-moving typhoons need much deeper subsurface layer, for example, D26 ~ 115-140m and UOHC ~ 115-125 kj cm^{-2} are needed for travelling at $U_h \sim$ 2-3 ms^{-1}. Ocean mixed layer numerical experiments and air-sea enthalpy flux estimation support the above observations that though over relatively shallow layer, there is still sufficient flux for intensification since the negative feedback from cyclone's self-induced cooling (Price 1981; Emanuel 1999) can still be effectively restrained under fast translation speed. On the contrary, as the negative feedback is much enhanced when a storm is slow-moving (Price 1981; Lin et al. 2003a,b), a much deeper subsurface warm layer is required for slow-moving typhoons.

Given the above observed strong dependence between translation speed and the subsurface parameters, in this work, a new concept named the 'affordable minimum translation speed (U_{h_min})' is

proposed. This is the minimum speed a storm has to travel to keep the self-induced cooling negative feedback restrained within a certain threshold during the intensification process to category 5, given the observed D26 or UOHC. Using more than 3,000 Argo profiles (Gould et al. 2004; Roemmich et al. 2004), a series of mixed layer model experiments are conducted to quantify the relationships between D26 (UOHC) and U_{h_min}. Linear relationships with correlation coefficients R = -0.87 (-0.71) are obtained as $U_{h\_min} = -0.065 \times D26 + 11.1$, and $U_{h\_min} = (-0.05 \times UOHC) + 9.4$, respectively. As both relationships are linear, they can in turn be used to estimate the minimum required D26 and UOHC, given the observed U_h, i.e., $D26_{\_min} = -11.7 \times U_h + 155$ and $UOHC_{\_min} = -10.1 \times U_h + 142$. Typically, for U_h = 1-3, 4-6, and 7-9 ms^{-1}, the corresponding average $D26_{\_min}$ ($UOHC_{\_min}$) is about 124-144m (116-122 kj cm^{-2}), 76-107m (75-104 kj cm^{-2}), and 56-68m (56-66 kj cm^{-2}), respectively.

Finally, the findings in this work are consolidated with the results in Part I (Lin et al. 2008a) and the relationship with ocean features and suggestion for future forecast reference is made.

References

Black, P. G., E. A. D'Asaro, W. M. Drennan, J. R. French, P. P. Niller, T. B. Sanford, E. J. Terrill, E. J. Walsh, and J. A. Zhang, 2007: Air-sea exchange in hurricanes, *Bull. Amer. Meteor. Soc.,* 88, 357-374.

Cione, J. J., and E. W. Uhlhorn, 2003: Sea surface temperature variability in hurricanes: Implications with respect to intensity change. *Mon. Wea. Rev.,* 131, 1783-1796.

Emanuel, K. A., 1995: Sensitivity of tropical cyclones to surface exchange coefficients and a revised steady-state model incorporating eye dynamics. *J. Atmos. Sci.*, 52, 3969-3976.

Emanuel, K. A., 1997: Some aspects of hurricane inner-core dynamics and energetics. *J. Atmos. Sci.*, 54, 1014-1026.

Emanuel, K. A., 1999: Thermodynamic control of hurricane intensity. *Nature,* 401, 665-669.

Emanuel, K. A., C. DesAutels, C. Holloway, and R. Korty, 2004: Environmental control of tropical cyclone intensity. *J. Atmos. Sci.,* 61, 843–858.

Emanuel, K., 2005: Increasing destructiveness of tropical cyclones over the past 30 years. *Nature*, 436,

686-688.

Frank, W. M., and E. A. Ritchie, 2001: Effects of vertical wind shear on the intensity and structure of numerically simulated hurricanes. *Mon. Wea. Rev.*, 129, 2249-2269.

Gallacher, P. C., R. Rotunno, and K. A. Emanuel, 1989: Tropical cyclogenesis in a coupled ocean-atmosphere model. Preprints of the 18th Conf. on Hurricanes and Trop. Meteor., *Amer. Meteor. Soc.*, Boston.

Goni, G. J., S. Kamholtz, S. Garzoli, and D. B. Olson, 1996: Dynamics of the Brazil–Malvinas confluence based upon inverted echo sounders and altimetry. *J. Geophys. Res.,* 101 (7), 16273–16289.

Goni, G. J., and J. A. Trinanes, 2003: Ocean thermal structure monitoring could aid in the intensity forecast of tropical cyclones. *EOS, Trans. Amer. Geophys. Union,* 84, 573-580.

Gould, J., D. Roemmich, S. Wijffels, H. Freeland, M. Ignaszewesky, X. Jianping, S. Pouliquen, Y. Desaubies, U. Send, K. Radhakrishnan, K. Takeuchi, K. Kim, M. Danchenkov, P. Sutton, B. King, B. Owens, and S. Riser, 2004: Argo Profiling Floats Bring New Era of In Situ Ocean Observations. *EOS, Trans. Amer. Geophys. Union,* 85, 179&190-191.

Gray, W. M., 1977: Tropical cyclone genesis in the western North Pacific. *J. Meteor. Soc. Japan (Ser. II)*, 55, 465-482.

Gray, W. M., 1979: Hurricanes: Their formation, structure and likely role in the tropical circulation. *Meteorology over the Tropical Oceans,* D. B. Shaw, Ed., Royal Meteorological Society, 155–218.

Holliday, C. R., and A. H. Thompson, 1979: Climatological characteristics of rapidly intensifying typhoons. *Mon. Wea. Rev.*, 107, 1022-1034.

Houze, R. A. Jr., S. S. Chen, B. F. Smull, W. C. Lee, and M. M. Bell, 2007: Hurricane intensity and eyewall replacement, *Science*, 315, 1235–1239.

Jacob, S. D., L. K. Shay, A. J. Mariano, and P. G. Black, 2000: The 3D oceanic mixed layer response to hurricane Gilbert. *J. Phys. Oceanogr.,* 30, 1407-1429.

Johnson, G. C., S. Levitus, J. M. Lyman, C. Schmid, and J. Willis, 2006: Ocean heat content variability, in

NOAA Annual report on the state of the ocean and the ocean observing system for climate, 74- 84.

Keeley, B., C. Sun, and L. P. Villeon, 2003: Global Temperature and Salinity Profile Program Annual Report. *NOAA/National Oceanographic Data Center*, Silver Spring, MD.

Leipper, D., and D. Volgenau, 1972: Hurricane heat potential of the Gulf of Mexico. *J. Phys. Oceanogr.,* 2, 218-224.

Lin, I I, W. T. Liu, C. C. Wu, J. C. H. Chiang, and C. H. Sui, 2003a: Satellite observations of modulation of surface winds by typhoon-induced upper ocean cooling. *Geophys. Res. Lett.,* 30, 1131, doi:10.1029/2002GL015674.

Lin, I I, W. T. Liu, C. C. Wu, G. T. F. Wong, C. Hu, Z. Chen, W. D. Liang, Y. Yang, and K. K. Liu, 2003b: New evidence for enhanced ocean primary production triggered by tropical cyclone. *Geophys. Res. Lett.,* 30, 1718, doi:10.1029/2003GL017141.

Lin, I I, C. C. Wu, K. A. Emanuel, I. H. Lee, C. R. Wu, and I. F. Pun, 2005: The Interaction of Supertyphoon Maemi (2003) With a Warm Ocean Eddy. *Mon. Wea. Rev.,* 133, 2635-2649.

Lin, I I, C. C. Wu, I. F. Pun, and D. S. Ko, 2008a: Upper Ocean Thermal Structure and the Western North Pacific Category-5 Typhoons, Part I: Ocean Features and Category-5 Typhoon's Intensification, *Mon. Wea. Rev.*, 136, 3288-3306..

Lin, I I, C. H. Chen, I. F. Pun, W. T. Liu, and C. C. Wu, 2008b: Warm ocean anomaly, air-sea fluxes, and the rapid intensification of tropical cyclone Nargis (2008). *Geophys. Res. Lett.,* in press.

Lyman, J. M., J. K. Willis, G. C. Johnson, 2006: recent cooling in the upper ocean, *Geophys. Res. Lett.*, 33, L18604, doi: 10.1029/2006GL027033.

Mainelli, M., M. DeMaria, L. K. Shay, and G. Goni, 2008: Application of oceanic heat content estimation to operational forecasting of recent Atlantic category 5 hurricanes. *Wea. Forecasting*, 23(1):3-16.

Merrill, R., 1988: Characteristics of the upper-tropospheric environmental flow around hurricanes. *J. Atmos. Sci.*, 45, 1665-1677.

Millero, F. J., C. T. Chen, A. Bradshaw, and K. Schleicher, 1980: A new high pressure equation of state for seawater. *Deep Sea Res.*, 27A, 255-264.

Montgomery, M. T., M. M. Bell, S. D. Aberson, and M. L. Black, 2006: Hurricane Isabel (2003): New insights into the physics of intense storms. Part I: Mean vortex structure and maximum intensity estimates. *Bull. Amer. Meteor. Soc.*, 87, 1335-1347.

Perlroth, I., 1967, Hurricane ehavior as related to oceanographic environmental conditions. *Tellus*, 19, 258-268.

Powell, M. D., P. J. Vickery, and T. A. Reinhold, 2003: Reduced drag coefficient for high wind speeds in tropical cyclones. *Nature*, 422, 279-283.

Price, J. F., 1981: Upper ocean response to a hurricane. *J. Phys. Oceanogr.,* 11, 153–175.

Price, J. F., R. A. Weller, and R. Pinkel, 1986: Diurnal cycling: Observations and models of the upper ocean response to diurnal heating, cooling, and wind mixing. *J. Geophys. Res.*, 91, 8411-8427.

Pun, I. F., I I Lin, C. R. Wu, D. S. Ko, and W. T. Liu, 2007: Validation and Application of Altimetry-derived Upper Ocean Thermal Structure in the Western North Pacific Ocean for Typhoon Intensity Forecast. *IEEE Trans. Geosci. Remote Sens.*, 45, 6, 1616-1630.

Roemmich, D., S. Riser, R. Davis, and Y. Desaubies, 2004: Autonomous profiling floats: Workhorse for broadscale ocean observations. *J. Mar. Technol. Soc*, 38, 31-39.

Shay, L. K., G. J. Goni, and P. G. Black, 2000: Effects of a warm oceanic feature on Hurricane Opal. *Mon. Wea. Rev.*, 128, 1366-1383.

Stephens, C., Antonov, J. I., Boyer T. P., Conkright M. E., Locarnini R. A., O'Brien TD, Garcia HE. 2002: World Ocean Atlas 2001 Volume 1: Temperature, S. Levitus, Ed., NOAA Atlas NESDIS 49. *U. S. Government Printing Office*, Washington, D. C.

Trenberth, K., 2005: Uncertainty in hurricanes and global warming, *Science,* 308, 1753-1754.

Trenberth, K., 2006: The role of the oceans in climate, in NOAA Annual report on the state of the ocean and the ocean observing system for climate. *NOAA Climate Program Office,* Silver Spring, MD. 27-33.

Vecchi, G. A., and B. J. Soden, 2007: Effect of remote sea surface temperature change on tropical cyclone potential intensity. *Nature*, 450(7172), 1066-1070.

Vimont, D. J., and J. P. Kossin, 2007: The Atlantic meridional mode and hurricane activity. *Geophys. Res. Lett.*, 34, L07709, doi:10.1029/2007GL029683.

UNESCO 1983: Algorithms for computation of fundamental properties of seawater. *Unesco Tech. Pap. in Mar. Sci*. 44, 53.

Wang, Y., and C. C. Wu, 2003: Current understanding of tropical cyclone structure and intensity changes - A review. *Meteor. Atmos. Phys.*, 87, 257-278, DOI: 10.1007/s00703-003-0055-6.

Wentz F. J., C. Gentemann, D. Smith, D. Chelton, 2000: Satellite measurements of sea surface temperature through clouds. *Science*, 288, 5467, 847-850.

Willis, J. K., J. M. Lyman, G. C. Johnson, and J. Gilson, 2007: Correction to 'Recent Cooling of the upper ocean', *Geophys. Res. Lett.*, 34, L16601, doi:10.1029/2007GL030323.

Wu, C.-C., C.-Y Lee, and I-I Lin, 2007: The effect of the ocean eddy on tropical cyclone intensity. *J. Atmos. Sci.*, 64, 3562-3578.

Acknowledgements

The authors wish to thank Prof. Dong-Ping Wang for providing the mixed layer model, to Mr. Chi Hong Chen for data processing, to the Reviewers for the valuable comments. Thanks also to the Joint Typhoon Warning Center, Remote Sensing System, NASA Jet Propulsion Lab, NOAA/GTSPP and the Argo float teams for data provision. This work is supported by the National Science Council, Taiwan through NSC97-2111-M-002-014-MY3, NSC 95-2611-M-002-024-MY3, and the joint programme between Taiwan National Science Council's Integrated Typhoon-Ocean Program (ITOP) and the US Office of Naval Research's Typhoon DRI Program.

Table captions:

Table 1: The mean (std) of the observed pre-storm SST, D26, UOHC, together with the minimum, maximum, and the averaged observed translation speed for each of the 5 groups.

Table 2: The during storm self-induced SST cooling estimated from the PWP model (Price et al. 1986) for each group at various intensification periods.

Table 3: Look-up table of the required minimum D26 (i.e., $D26\_{min}$) under various translation speeds based on Fig. 7c.

Table 4: Look-up table of the required minimum UOHC (i.e., $UOHC\_{min}$) under various translation speeds based on Fig. 9c.

Figure Captions:

Fig. 1: (a) The searched pre-storm *in situ* depth-temperature profiles found in the intensification locations. The profiles are sorted into 5 groups, according to the D26. (b) The corresponding observed translation speed for each group.

Fig. 2: Results from the PWP mixed layer numerical experiments showing the during-storm inner-core SST at various intensification periods for each of the 5 groups.

Fig. 3: Corresponding to Fig. 2, the during-storm depth-temperature profiles for each of the 5 groups at various intensification periods.

Fig. 4: The averaged self-induced ocean cooling negative feedback estimated using the PWP model for each of the 5 groups under progressively increase wind forcing (every 5 m s^{-1} interval) from category 1 to 5. For each group, self-induced cooling is estimated at various translation speeds (i.e., U_h= 1,2,3,…10 m s^{-1}) and the observed range of *Uh* is shaded in dark grey.

Fig. 5: Corresponding to Fig. 4, the estimated averaged enthalpy flux for each of the 5 groups during the intensification period from category-1 to 5. For each group, enthalpy flux is estimated at various translation speeds (i.e., U_h= 1,2,3,…10 m s^{-1}) and the observed range of *Uh* is shaded in dark grey. Also, region of enthalpy flux below 0 is shaded in light grey, indicating unsuitable condition for intensification.

Fig. 6: (a) 2 example profiles showing similar SST (both ~ 29.7°C) but of different warm layer thickness, one over shallow D26 of 67m (Profile 1) and the other over deep D26 of 134m (Profile 2). (b) The estimated self-induced ocean cooling at various translation speeds for Profile 1 with U_{h_min} indicated. Region of cooling confined within the 2.2°C threshold is shaded in light grey, indicating possible condition for intensification. (c) same as in (b), but for Profile 2.

Fig. 7: (a) The D26-U_{h_min} relationship obtained from the 17 profiles in Fig. 1a. (b) same as (a), but obtained from the 3326 profiles in Fig. 8b with the 17 pairs in (a) overlaid (colour scheme for each group see Fig. 1a). (c) as in (b), but for the U_h - D26$_{_min}$ relationship.

Fig. 8: (a) Locations (in grey) of the 3326 Argo *in situ* profiles searched from the region between

120-170°E and 10-26°N during the May-October typhoon season between 2000 and 2006. The location of the profiles in Fig. 1a are overlaid and depicted in black. (b) The depth-temperature distribution of the 3326 profiles (in grey) with the profiles in Fig. 1a overlaid (in black).

Fig. 9: (a) The dependence between D26 and UOHC. (b) The UOHC-U_{h_min} relationship obtained from the 3326 profiles in Fig. 8b. (c) The U_h - UOHC$_{_min}$ relationship for the 3326 profiles in Fig. 8b.

Fig. 10: The corresponding U_{h_min} (annotated in stars) for various background D26 (based on eqn. 3). Also, range of U_h where encountering +SSHA feature is needed is depicted in blue arrows, while range of U_h where encountering +SSHA feature is not needed is depicted in green arrows. The applicable range of the background D26 for the 3 sub-regions (i.e., SEZ, Kuroshio, and gyre central) in the western North Pacific, as identified in Part I, is also depicted for reference.

Fig. 11: (a) The D26- U_{h_mean} pairs obtained using the mean self-induced cooling of 1.6°C with the regression relationship depicted in black-solid line. The regression relationship from Fig. 7b is depicted in brown-solid line for reference. The actual observed 17 U_h – D26 pairs in the past 10 years are depicted in colour (colour scheme for each group see Fig. 1a) with the regression relationship derived using these actual observations in black-dashed line. (b) As in (a), but for the U_h - D26$_{_min}$ pairs.

Fig. 12: (a) The U_h - D26$_{_min}$ relationship under the small-regular N2 condition (i.e., N2 $\leqq$ $4x10^{-4}S^{-2}$). (b) as in (a) but under the large N2 (i.e., N2 > $4x10^{-4}S^{-2}$) condition.

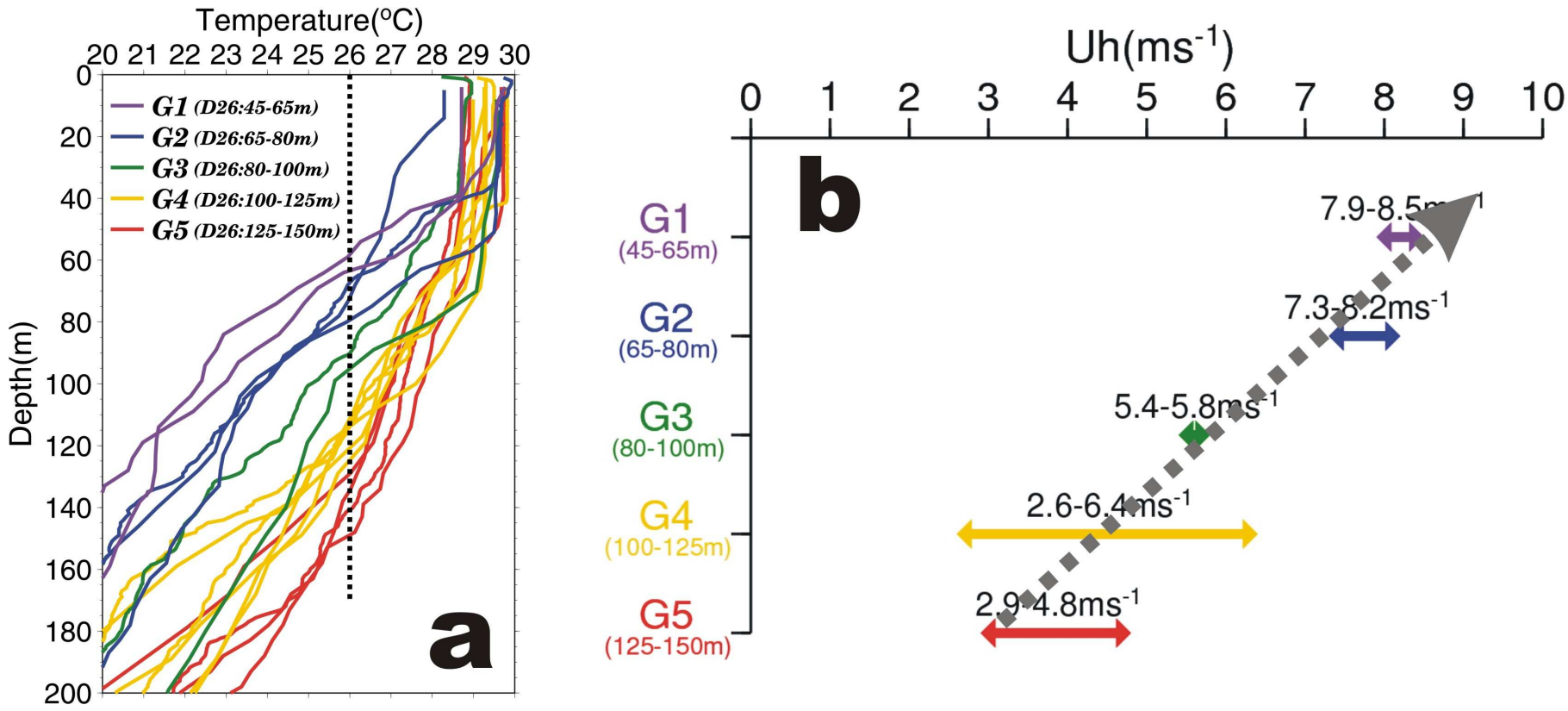

Fig. 1: (a) The searched pre-storm *in situ* depth-temperature profiles found in the intensification locations. The profiles are sorted into 5 groups, according to the D26. (b) The corresponding observed translation speed for each group.

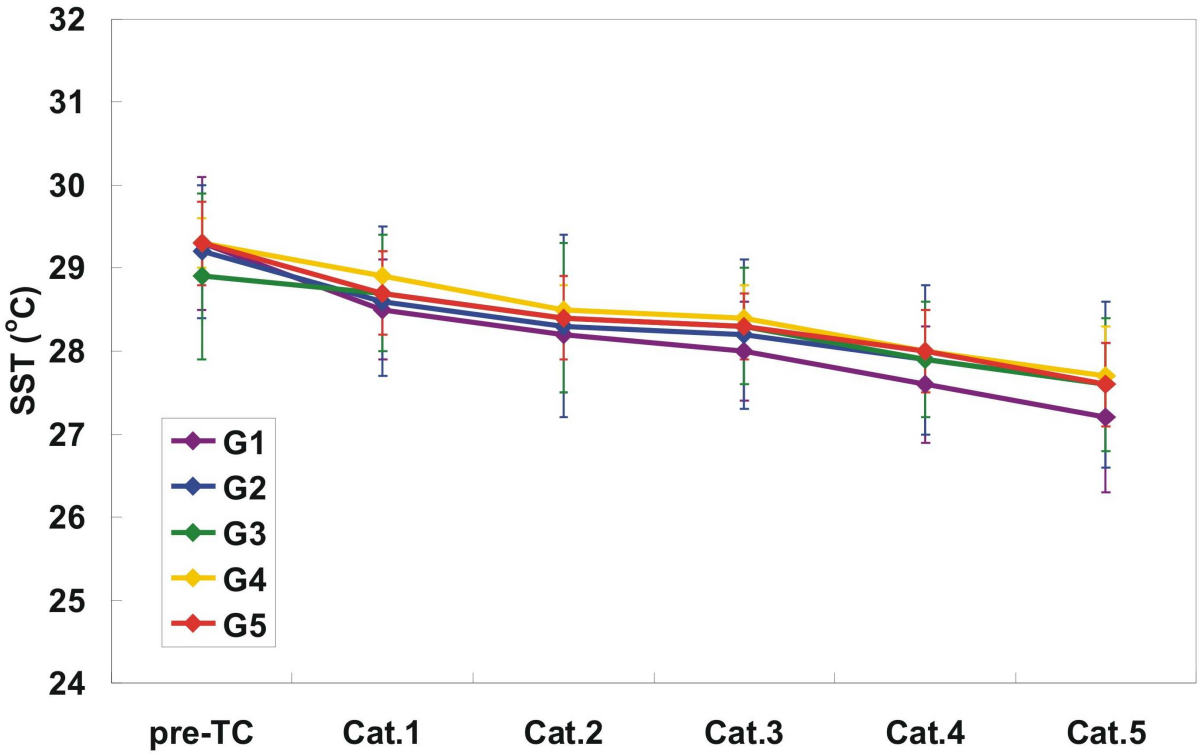

Fig. 2: Results from the PWP mixed layer numerical experiments showing the during-storm inner-core SST at various intensification periods for each of the 5 groups.

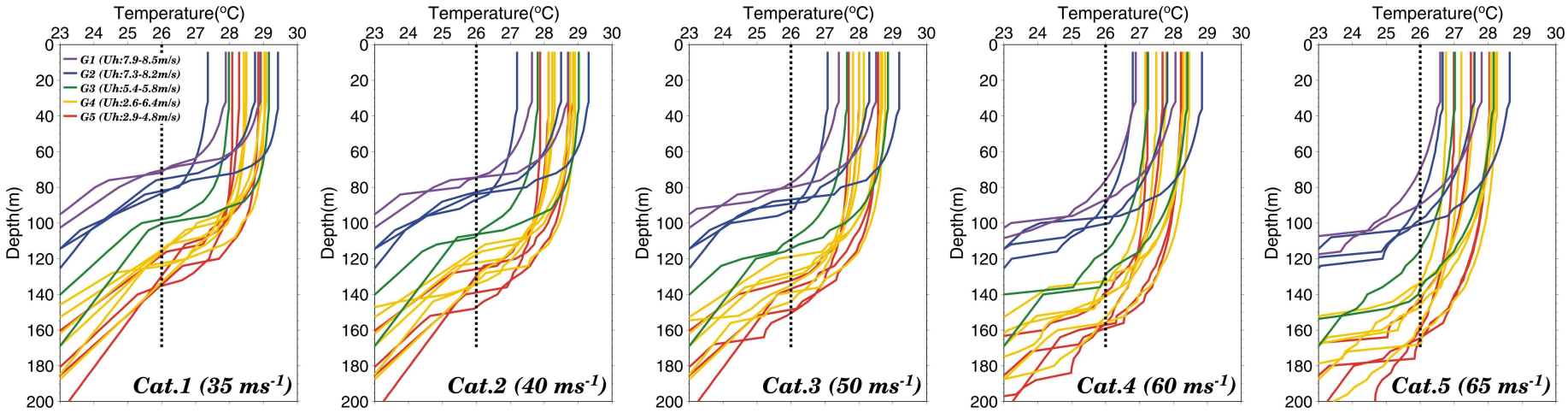

Fig. 3: Corresponding to Fig. 2, the during-storm depth-temperature profiles for each of the 5 groups at various intensification periods.

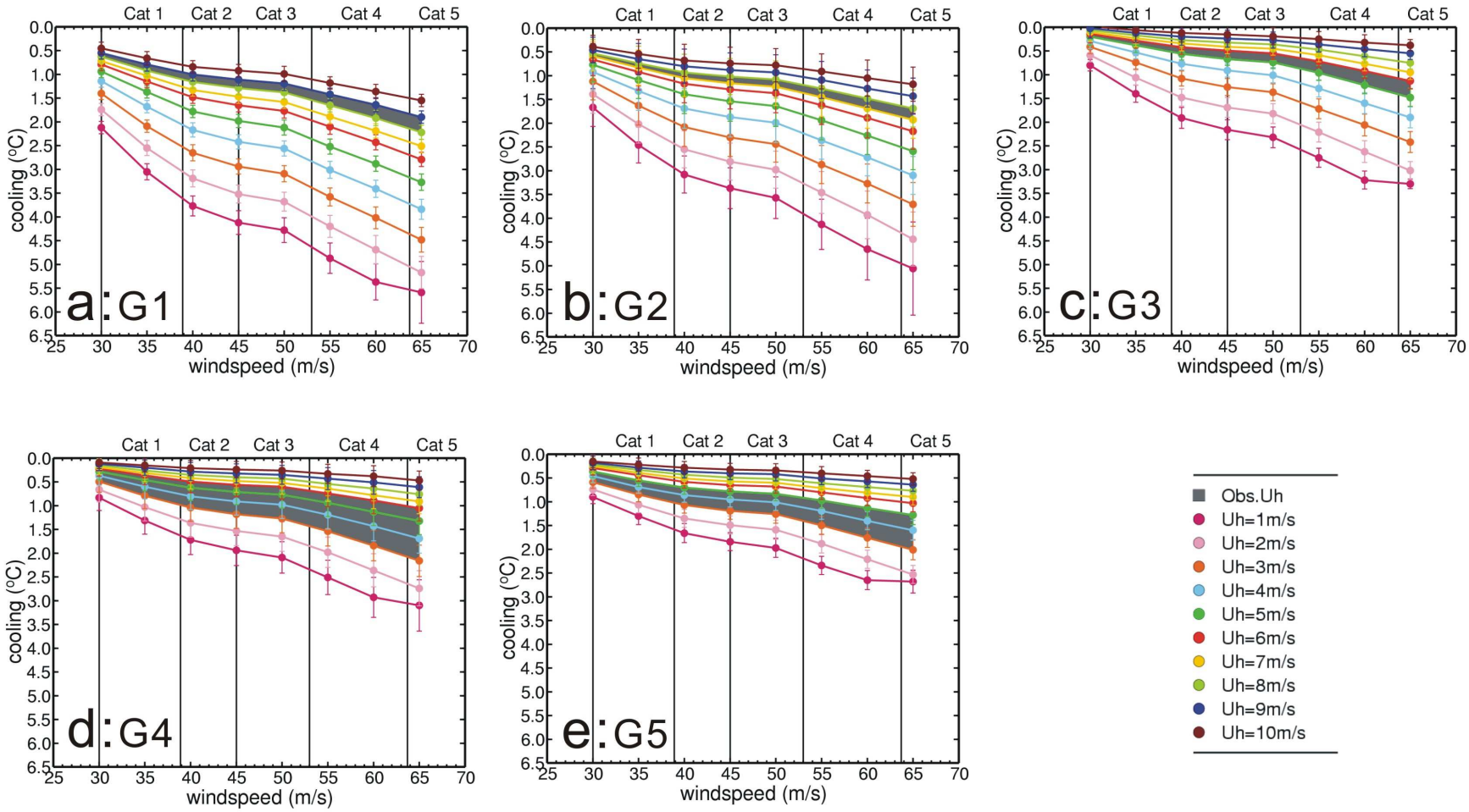

Fig. 4: The averaged self-induced ocean cooling negative feedback estimated using the PWP model for each of the 5 groups under progressively increase wind forcing (every 5 m s-1 interval) from category 1 to 5. For each group, self-induced cooling is estimated at various translation speeds (i.e., *Uh*= 1,2,3,…10 m s-1) and the observed range of *Uh* is shaded in dark grey.

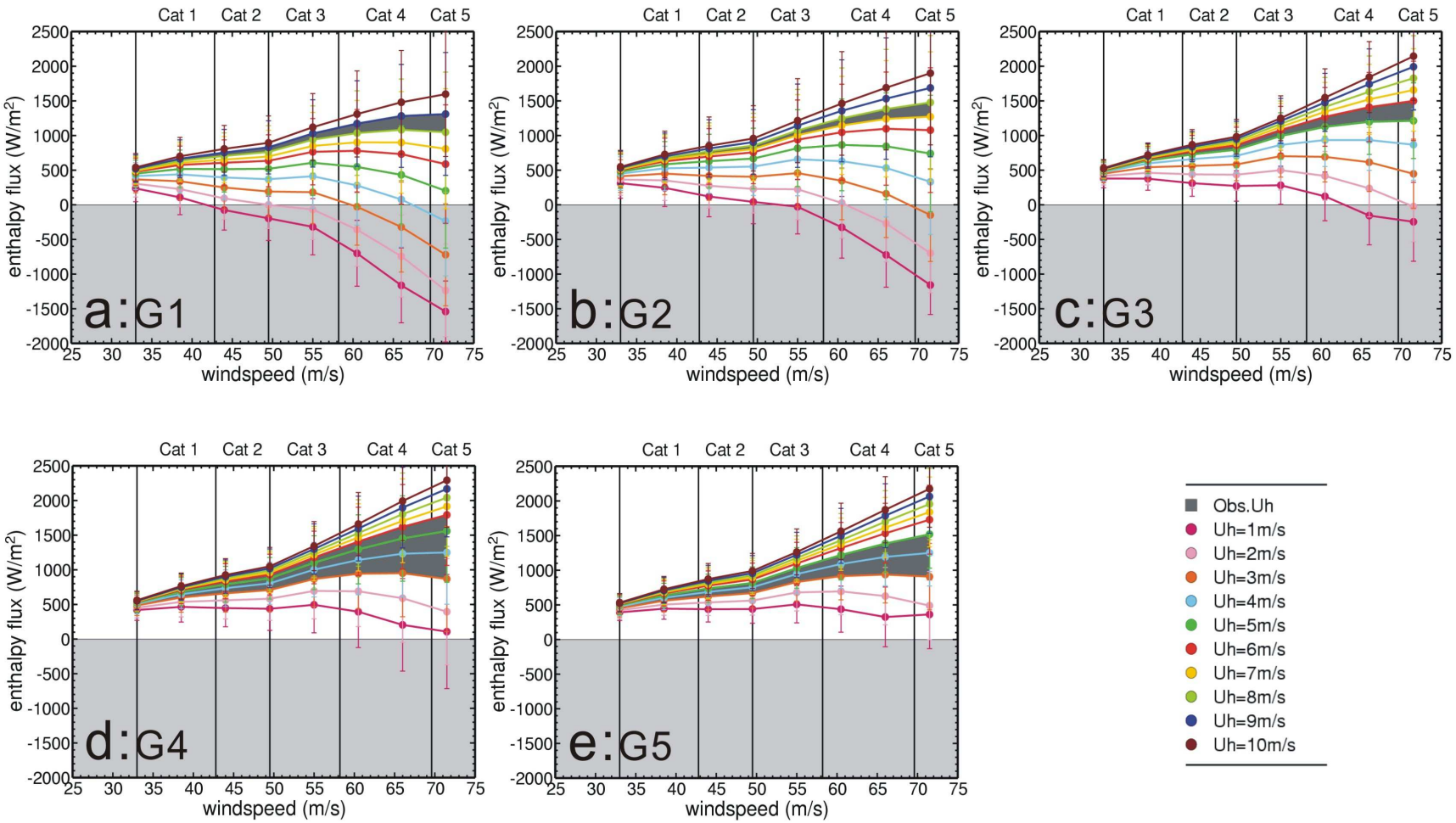

Fig. 5: Corresponding to Fig. 4, the estimated averaged enthalpy flux for each of the 5 groups during the intensification period from category-1 to 5. For each group, enthalpy flux is estimated at various translation speeds (i.e., *Uh*= 1,2,3,…10 m s-1) and the observed range of *Uh* is shaded in dark grey. Also, region of enthalpy flux below 0 is shaded in light grey, indicating unsuitable condition for intensification.

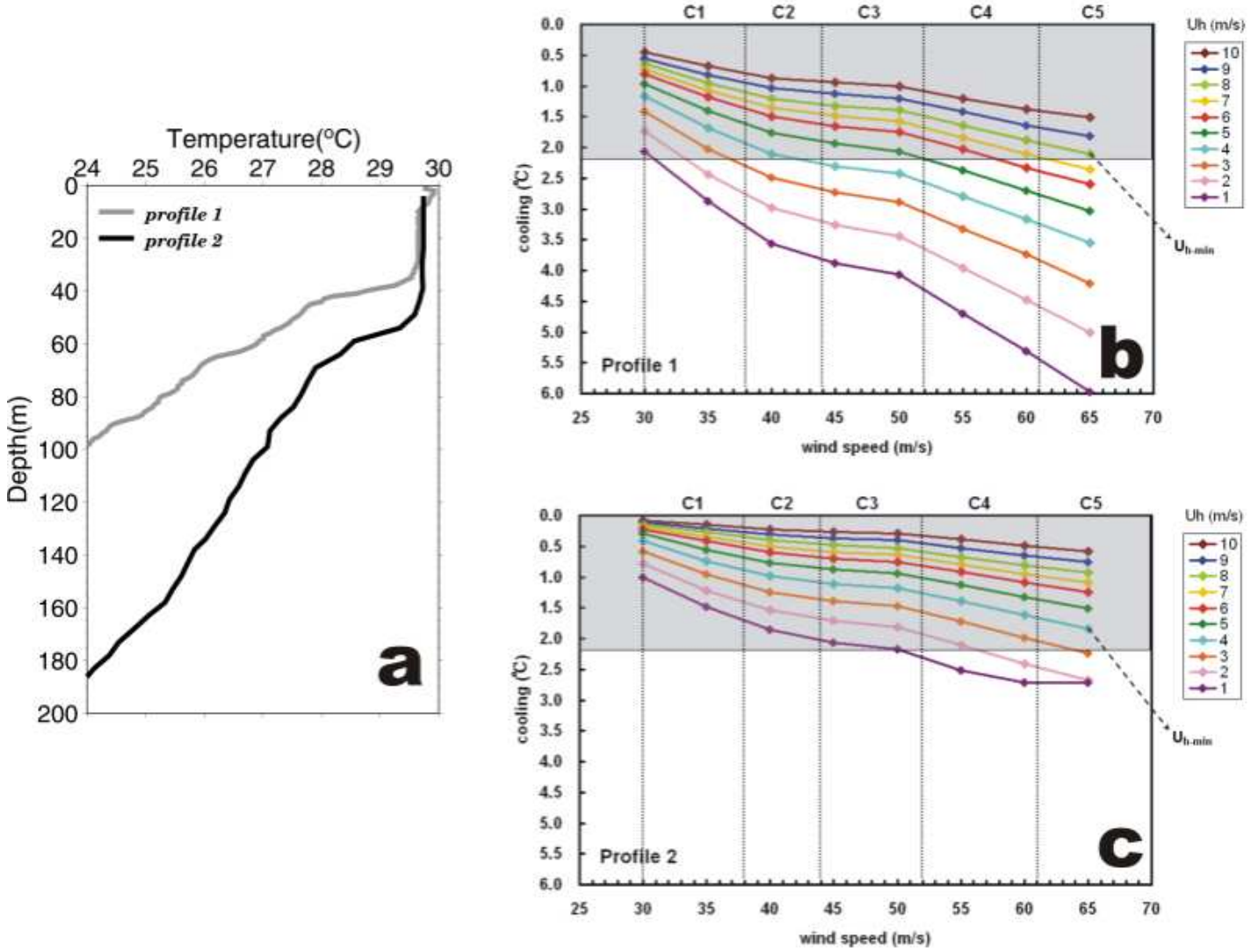

Fig. 6: (a) 2 example profiles showing similar SST (both ~ 29.7°C) but of different warm layer thickness, one over shallow D26 of 67m (Profile 1) and the other over deep D26 of 134m (Profile 2). (b) The estimated self-induced ocean cooling at various translation speeds for Profile 1 with *Uh_min* indicated. Region of cooling confined within the 2.2°C threshold is shaded in light grey, indicating possible condition for intensification. (c) same as in (b), but for Profile 2.

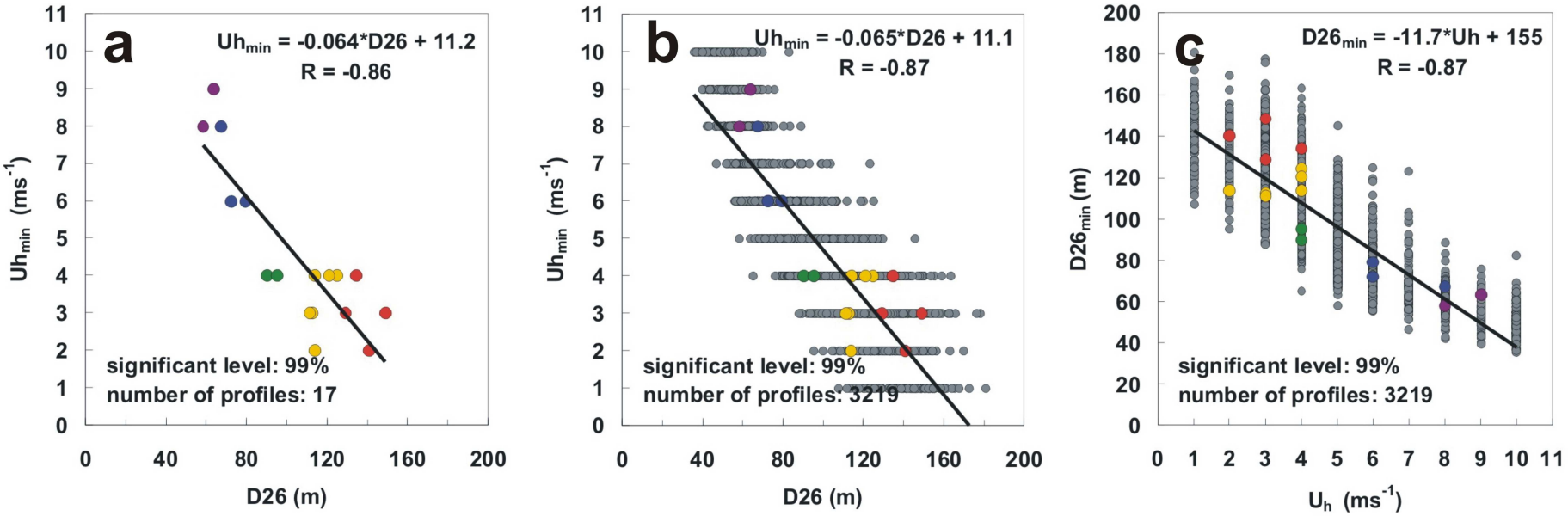

Fig. 7: (a) The D26-*Uh_min* relationship obtained from the 17 profiles in Fig. 1a. (b) same as (a), but obtained from the 3326 profiles in Fig. 8b with the 17 pairs in (a) overlaid (colour scheme for each group see Fig. 1a). (c) as in (b), but for the *Uh* - D26_*min* relationship.

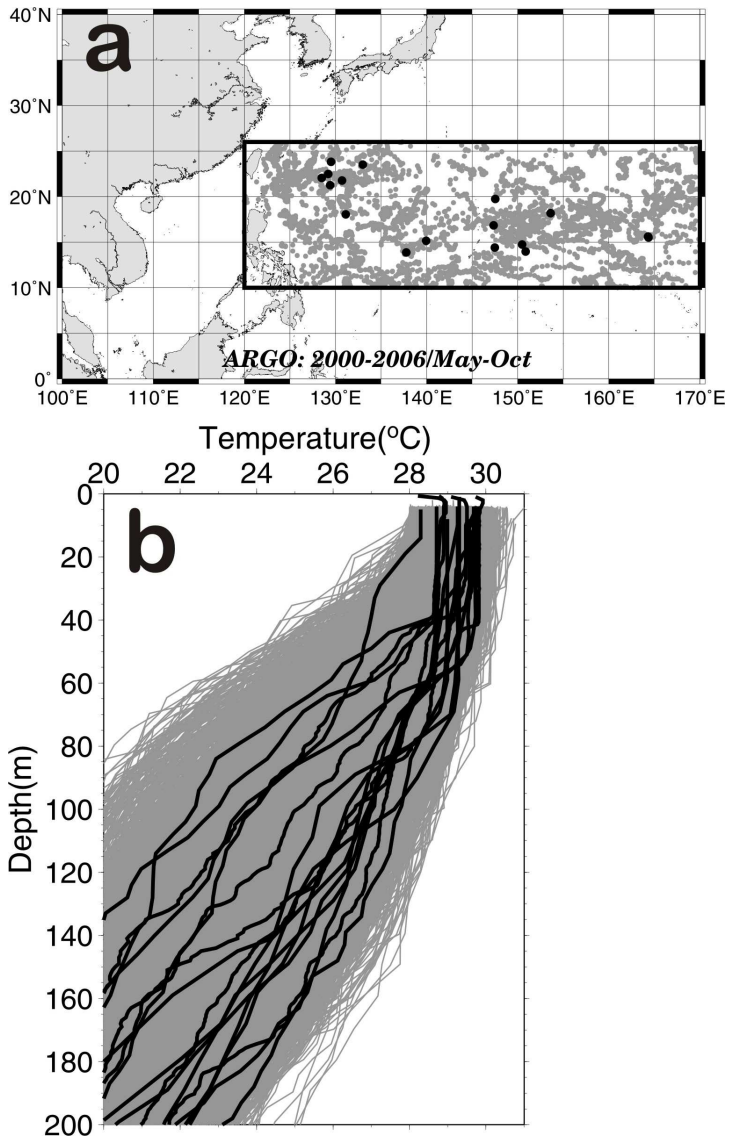

Fig. 8: (a) Locations (in grey) of the 3326 Argo *in situ* profiles searched from the region between 120-170°E and 10-26°N during the May-October typhoon season between 2000 and 2006. The location of the profiles in Fig. 1a are overlaid and depicted in black. (b) The depth-temperature distribution of the 3326 profiles (in grey) with the profiles in Fig. 1a overlaid (in black).

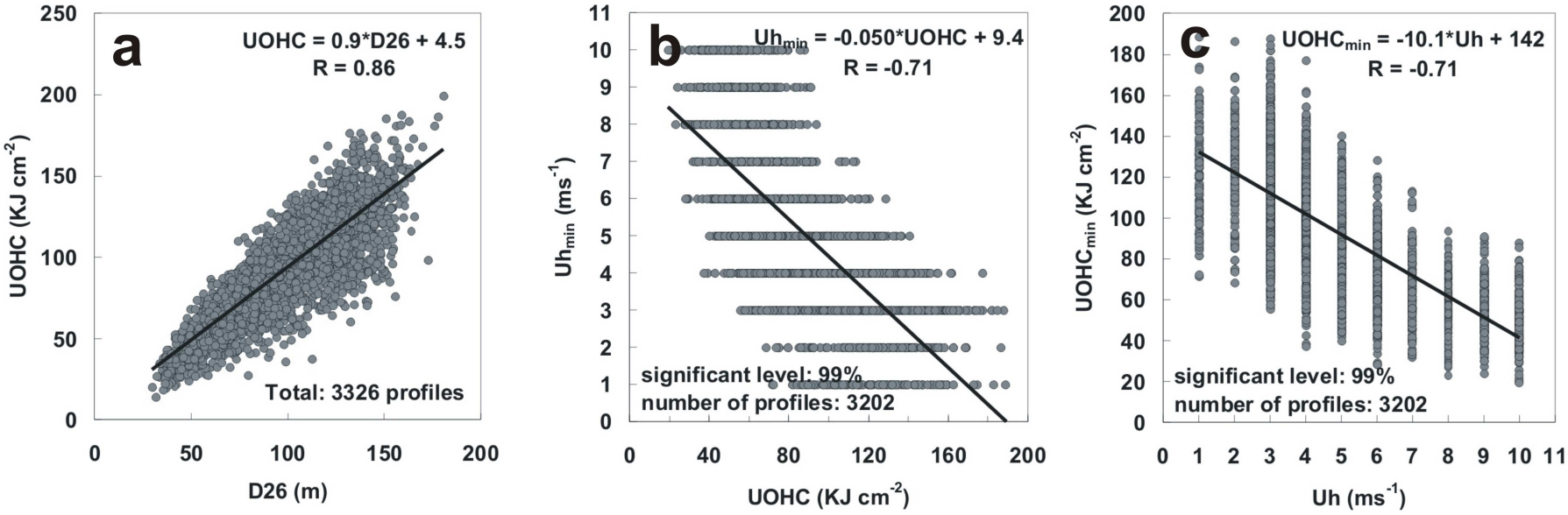

Fig. 9: (a) The dependence between D26 and UOHC. (b) The UOHC-*Uh_min* relationship obtained from the 3326 profiles in Fig. 8b. (c) The *Uh* - UOHC_*min* relationship for the 3326 profiles in Fig. 8b.

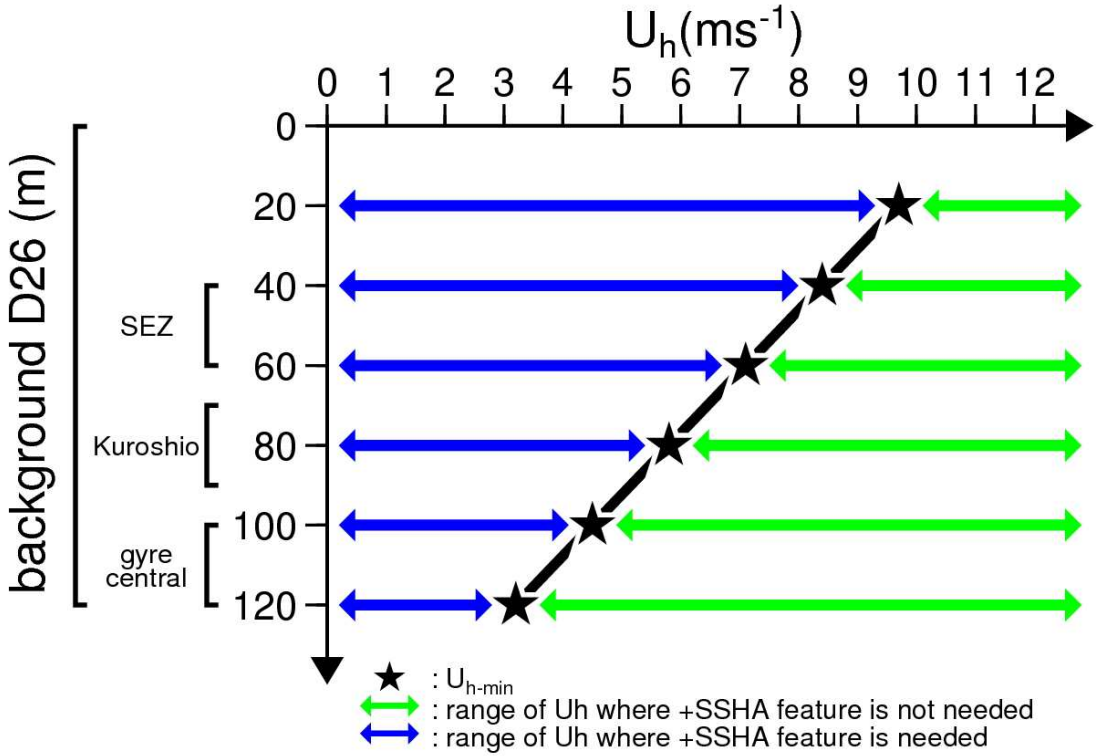

Fig. 10: The corresponding *Uh_min* (annotated in stars) for various background D26 (based on eqn. 3). Also, range of *Uh* where encountering +SSHA feature is needed is depicted in blue arrows, while range of *Uh* where encountering +SSHA feature is not needed is depicted in green arrows. The applicable range of the background D26 for the 3 sub-regions (i.e., SEZ, Kuroshio, and gyre central) in the western North Pacific, as identified in Part I, is also depicted for reference.

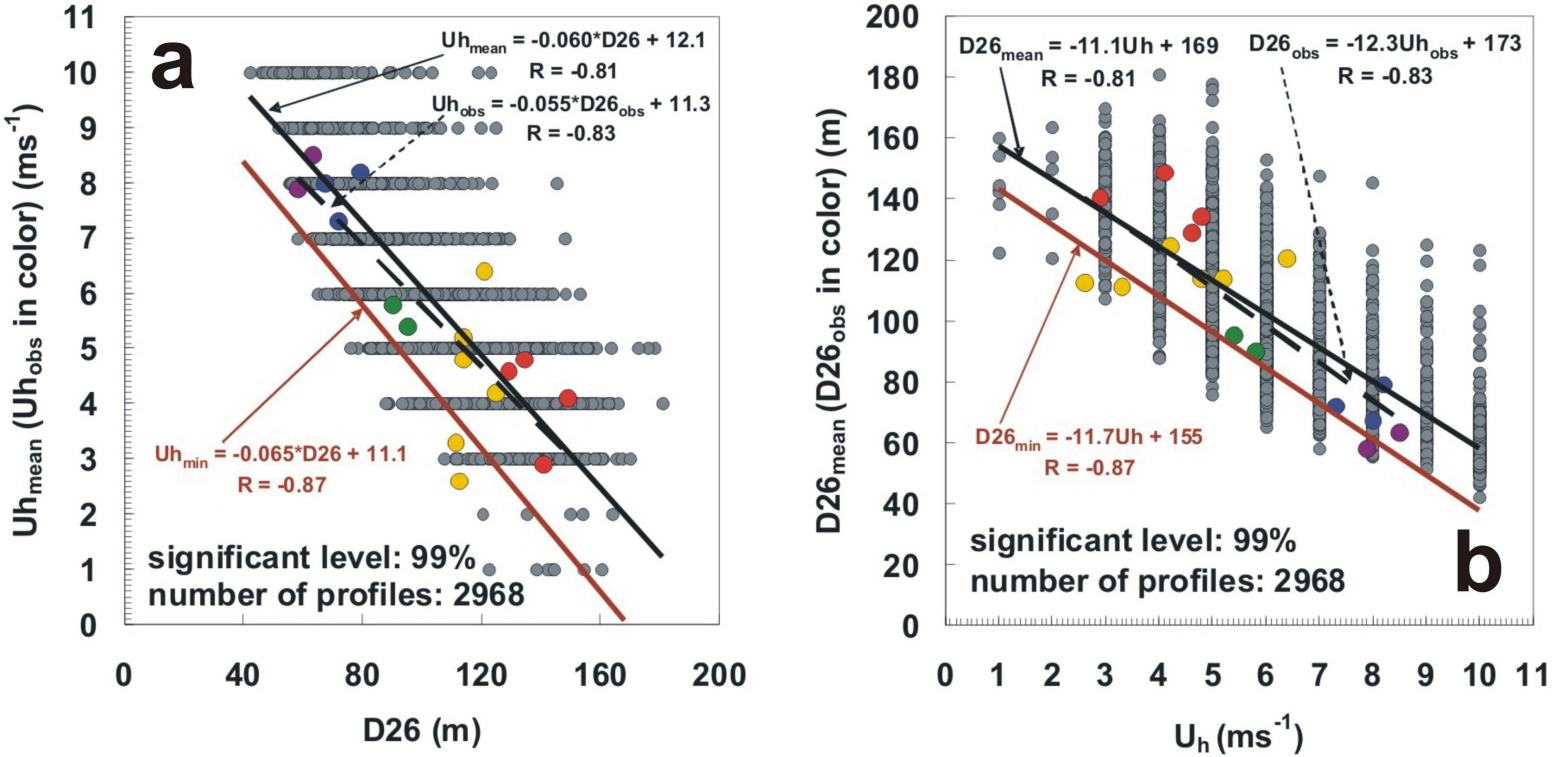

Fig. 11: (a) The D26- *Uh_mean* pairs obtained using the mean self-induced cooling of 1.6°C with the regression relationship depicted in black-solid line. The regression relationship from Fig. 7b is depicted in brown-solid line for reference. The actual observed 17 *Uh* – D26 pairs in the past 10 years are depicted in colour (colour scheme for each group see Fig. 1a) with the regression relationship derived using these actual observations in black-dashed line. (b) As in (a), but for the *Uh* - D26_*min* pairs.

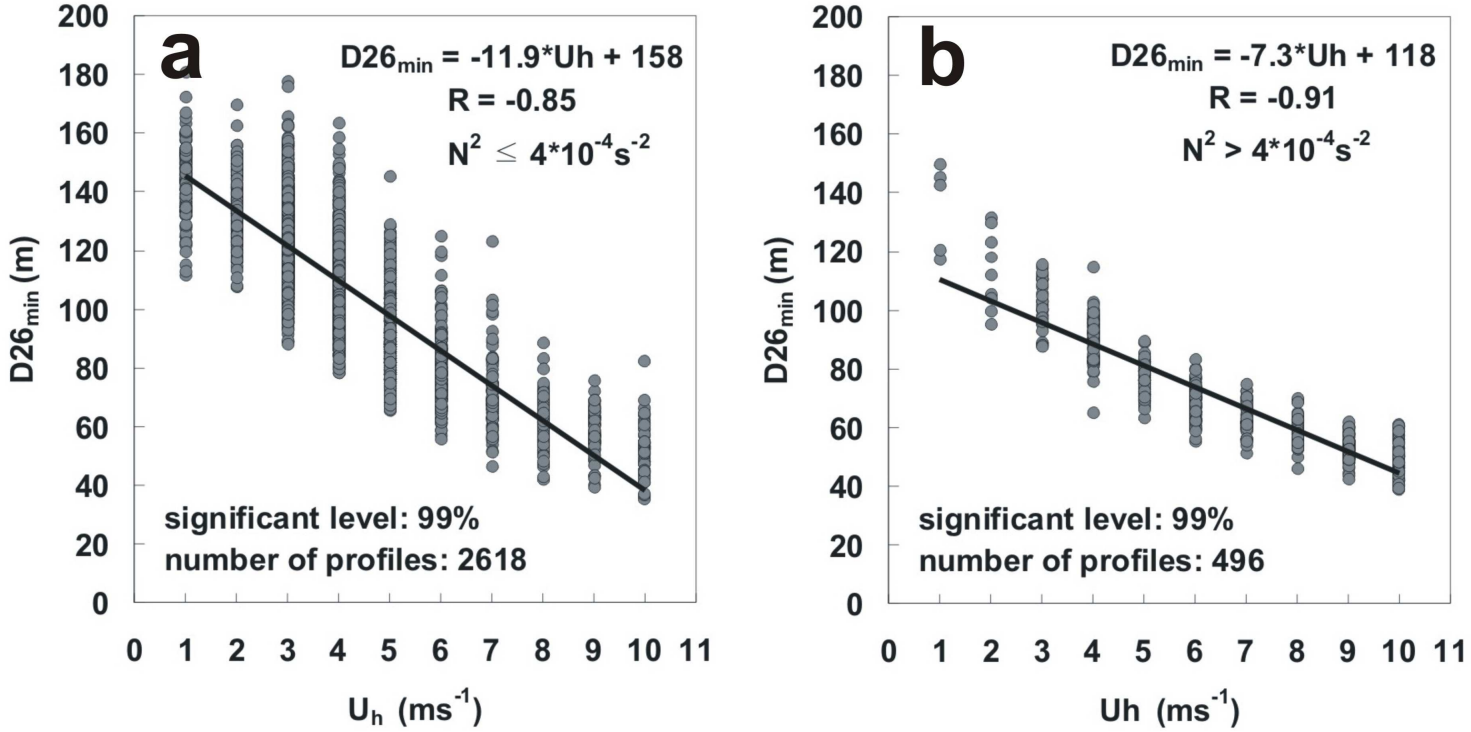

Fig. 12: (a) The *Uh* - D26_*min* relationship under the small-regular N2 condition (i.e., N2 $\leqq$ 4*x*10-4S-2). (b) as in (a) but under the large N2 (i.e., N2 > 4*x*10-4S-2) condition.

Table 1: The mean (std) of the observed pre-storm SST, D26, UOHC, together with the minimum, maximum, and the averaged observed translation speed for each of the 5 groups.

	Pre-SST(℃)	Pre-D26(m)	Pre-UOHC (kJ cm^{-2})	Min. Uh	Max. Uh	Ave. Uh
G1	29.3(0.8)	61(4)	64(15)	7.9	8.5	8.2(0.4)
G2	29.2(0.8)	73(6)	71 (31)	7.3	8.2	7.8(0.5)
G3	28.9(1.0)	93(4)	96 (32)	5.4	5.8	5.6(0.3)
G4	29.3(0.3)	116(5)	117 (10)	2.6	6.4	4.5(1.4)
G5	29.3(0.5)	138(9)	122 (18)	2.9	4.8	4.1(0.9)

Table 2: The during storm self-induced SST cooling estimated from the PWP model (Price et al. 1986) for each group at various intensification periods.

	pre-TC	Cat.1	Cat.2	Cat.3	Cat.4	Cat.5
G1		0.7(0.2)	1.1(0)	1.2(0.1)	1.7(0.1)	2.1(0.1)
G2		0.6(0.3)	0.9(0.4)	1.0(0.4)	1.3(0.5)	1.6(0.5)
G3		0.2(0.2)	0.5(0.1)	0.6(0.1)	1.0(0.2)	1.3(0.2)
G4		0.4(0.2)	0.8(0.3)	0.9(0.3)	1.3(0.4)	1.6(0.5)
G5		0.6(0.2)	0.9(0.1)	1.0(0.1)	1.3(0.2)	1.6(0.2)

Table 3: Look-up table of the required minimum D26 (i.e., *D26_min*) under various translation speeds based on Fig. 7c.

Uh (ms^{-1})	1	2	3	4	5	6	7	8	9	10
Mean D26 (m)	144	134	124	107	90	76	68	61	56	50
STD	13	13	15	15	14	11	11	8	7	7
Mean ± STD	131-157	121-147	109-139	92-122	76-104	65-87	57-79	53-69	49-63	43-57

Table 4: Look-up table of the required minimum UOHC (i.e., *UOHC_min*) under various translation speeds based on Fig. 9c.

Uh(ms^{-1})	1	2	3	4	5	6	7	8	9	10
Mean UOHC ($KJ\ cm^{-2}$)	122	122	116	104	89	75	66	58	56	50
STD	25	23	24	22	20	18	17	15	14	14
Mean ± STD	97-147	99-145	92-140	82-126	69-109	57-93	49-83	43-73	42-70	36-64